Metastatic castration-resistant prostate cancer reveals intrapatient similarity and interpatient heterogeneity of therapeutic kinase targets

Justin M. Drake[a], Nicholas A. Graham[b,c], John K. Lee[d,e], Tanya Stoyanova[a], Claire M. Faltermeier[e], Sudha Sud[f], Björn Titz[b,c], Jiaoti Huang[g,h,i], Kenneth J. Pienta[f,j], Thomas G. Graeber[b,c,g,k,l], and Owen N. Witte[a,c,l,m,1]

[a]Department of Microbiology, Immunology, and Molecular Genetics, [b]Crump Institute for Molecular Imaging, [c]Department of Molecular and Medical Pharmacology, [d]Division of Hematology and Oncology, Department of Medicine, [e]Molecular Biology Institute, [g]Jonsson Comprehensive Cancer Center, [h]Department of Pathology and Laboratory Medicine, [i]Eli and Edythe Broad Center of Regenerative Medicine and Stem Cell Research, [k]Institute for Molecular Medicine, [l]California NanoSystems Institute, and [m]Howard Hughes Medical Institute, David Geffen School of Medicine, University of California, Los Angeles, CA 90095; [j]The Brady Urological Institute, Johns Hopkins School of Medicine, Baltimore, MD 21231; and [f]Department of Internal Medicine, University of Michigan Medical School, Ann Arbor, MI 48109

Contributed by Owen N. Witte, October 23, 2013 (sent for review September 5, 2013)

In prostate cancer, multiple metastases from the same patient share similar copy number, mutational status, erythroblast transformation specific (ETS) rearrangements, and methylation patterns supporting their clonal origins. Whether actionable targets such as tyrosine kinases are also similarly expressed and activated in anatomically distinct metastatic lesions of the same patient is not known. We evaluated active kinases using phosphotyrosine peptide enrichment and quantitative mass spectrometry to identify druggable targets in metastatic castration-resistant prostate cancer obtained at rapid autopsy. We identified distinct phosphopeptide patterns in metastatic tissues compared with treatment-naive primary prostate tissue and prostate cancer cell line-derived xenografts. Evaluation of metastatic castration-resistant prostate cancer samples for tyrosine phosphorylation and upstream kinase targets revealed SRC, epidermal growth factor receptor (EGFR), rearranged during transfection (RET), anaplastic lymphoma kinase (ALK), and MAPK1/3 and other activities while exhibiting intrapatient similarity and interpatient heterogeneity. Phosphoproteomic analyses and identification of kinase activation states in metastatic castration-resistant prostate cancer patients have allowed for the prioritization of kinases for further clinical evaluation.

metastasis | resistance | personalized medicine | combination therapy | phosphotyrosine

Mutational and copy number analyses from epithelial tumors have identified several activating tyrosine kinase mutations and amplifications, such as epidermal growth factor receptor (EGFR) mutations in lung adenocarcinoma and erythroblastic leukemia viral oncogene homolog 2 (*ERBB2 or HER2/neu*) gene amplification in breast cancer (1). The dependence on these tyrosine kinases for tumor growth and survival has led to successful clinical treatment with tyrosine kinase inhibitors (TKIs) (2, 3). However, recent genomic analyses of prostate adenocarcinoma revealed that activating tyrosine kinase mutations or amplifications are very rare (1, 4–6).

Despite the scarcity of tyrosine kinase amplifications or activating mutations in prostate cancer, tyrosine kinase expression and activity has been shown to play an important role in disease progression. For example, coexpression of wild-type SRC tyrosine kinase and androgen receptor (AR) can synergistically drive the formation of mouse prostate adenocarcinoma (7). Evaluation of nontyrosine-kinase–initiated mouse models of prostate cancer further identified activation of the nonreceptor tyrosine kinases SRC, ABL1, and Janus kinase 2 (JAK2) (8). We also observed increased tyrosine phosphorylation in nearly 50% of castration-resistant prostate cancer (CRPC) tissues examined compared with hormone-naïve prostate cancer (8). These studies suggest that comprehensive evaluation of metastatic CRPC samples for tyrosine kinase activity may lead to the identification of new drug targets.

Studies in melanoma and breast cancer have revealed that despite heterogeneity in primary, localized disease, metastases seem to arise from a single precursor cell (9, 10). The multifocal nature of organ-confined prostate cancer poses a question as to the clonality of metastatic disease (11). Investigation into clonality in metastatic CRPC has found that tumors isolated from anatomically different lesions in the same patient bear similar copy number, mutational status, erythroblast transformation specific (ETS) rearrangements, and methylation patterns from multiple metastatic lesions supporting their clonal origins (6, 12–14). In addition, these studies found a remarkable amount of interpatient heterogeneity, suggesting that personalized medicine approaches may be necessary to efficiently target metastatic lesions. Previous observations of intrapatient similarity hold promise with regard to treatment strategies for metastatic CRPC patients by means of systematically attacking the cancer cell clone contributing to disease.

This led us to investigate whether actionable targets such as tyrosine kinases also maintain similar activation patterns across anatomically distinct metastases from the same patient. With

Significance

Metastatic castration-resistant prostate cancer (CRPC) remains incurable due to the lack of effective therapies. The need to identify new actionable targets in CRPC is crucial as we begin to examine the resistance mechanisms related to androgen withdrawal. Here, we report an unbiased quantitative phosphoproteomic approach to identify druggable kinases in metastatic CRPC. These kinase activation patterns revealed intrapatient similarity and interpatient heterogeneity across a large panel of targets. Interestingly, these kinase activities are not a result of mutation but rather pathway activation within the tumors themselves. The observation that similar kinase activities are present in most if not all anatomically disparate metastatic lesions from the same patient suggests that CRPC patients may benefit from individualized, targeted combination therapies.

Author contributions: J.M.D., N.A.G., K.J.P., T.G.G., and O.N.W. designed research; J.M.D., N.A.G., J.K.L., T.S., C.M.F., and S.S. performed research; J.M.D., N.A.G., J.K.L., C.M.F., B.T., and J.H. analyzed data; and J.M.D., N.A.G., J.K.L., and O.N.W. wrote the paper.

The authors declare no conflict of interest.

Freely available online through the PNAS open access option.

Data deposition: The MS proteomics data have been deposited in ProteomeXchange, www.proteomexchange.org (accession no. PXD000238).

[1]To whom correspondence should be addressed. E-mail: owenwitte@mednet.ucla.edu.

This article contains supporting information online at www.pnas.org/lookup/suppl/doi:10.1073/pnas.1319948110/-/DCSupplemental.

access to rare metastatic CRPC tissue from the University of Michigan's Rapid Autopsy Program (15), we evaluated global tyrosine phosphorylation patterns in lethal metastatic CRPC patients. Phosphotyrosine peptide enrichment and quantitative mass spectrometry (MS) identified diverse phosphorylation events in the metastatic tissues compared with naive primary prostate tissue and prostate cancer cell line-derived xenografts. Validation of activated kinases that were identified via either MS or kinase–substrate relationships revealed intrapatient similarity and interpatient heterogeneity across a large panel of targets. Interestingly, these kinase activities are a result not of mutation (6) but rather of pathway activation within the tumors themselves. In summary, the observation that similar tyrosine kinase activities are present in most if not all anatomically disparate metastatic lesions from the same patient reveals that (*i*) CRPC lesions may be clonal in origin and (*ii*) kinase activation patterns observed in these lesions should be prioritized for further evaluation as new targeted therapeutic strategies.

Results

Phosphotyrosine Peptide Signatures Are Dramatically Different Between Prostate Cancer Cell Line-Derived Xenografts and Treatment-Naïve or Metastatic CRPC Tissues. To identify and discover unique kinase targets in metastatic CRPC, we analyzed 16 metastatic CRPC samples from 13 different patients obtained at rapid autopsy (15) by quantitative label-free phosphotyrosine MS (Fig. 1). These included eight anatomically unique sites as well as two or three distinct sites from three separate patients. Each sample contained greater than 50% tumor content as determined by histological analyses. We also analyzed one benign prostatic hyperplasia (BPH), six treatment-naïve matched benign and cancerous prostates, and metastatic or s.c. xenograft tumors derived from the androgen-insensitive 22Rv1 and androgen-sensitive LNCaP cell lines (Dataset S1) (8). From three separate phosphotyrosine enrichment preparations and MS analyses, we identified 297 unique phosphopeptides corresponding to 185 unique proteins (Dataset S2).

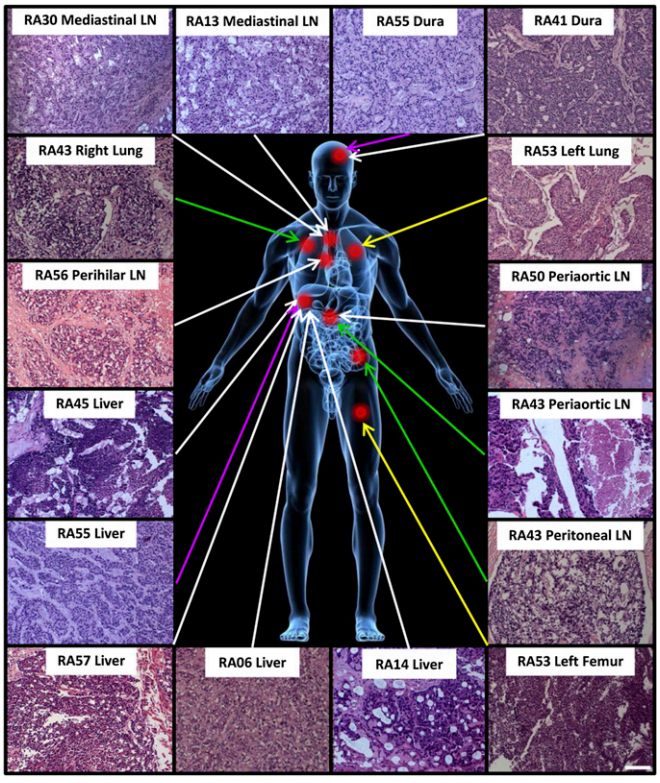

Fig. 1. Anatomical location and histological characterization of metastatic CRPC samples used for phosphoproteomics. Metastatic CRPC tissues were obtained from the Rapid Autopsy Program at the University of Michigan. Sixteen samples from 12 different patients are represented and prepared as previously described for phosphoproteomics (8). Red dots indicate the approximate location of the metastatic lesions analyzed. Same-colored lines represent tissues from the same patient. Patient RA53 left lung and left femur were combined due to limiting material (yellow lines). Only tissues with greater than 350 mg and 50% tumor content were evaluated. (Scale bar, 50 μm.)

To compare different models and stages of prostate cancer, we included cell line-derived xenografts, treatment-naïve primary prostate benign and cancerous tissues, and metastatic CRPC in a single phosphotyrosine enrichment preparation. Unsupervised hierarchical clustering revealed three separate clusters. In particular, the cell line-derived xenografts formed a distinct group compared to the primary tissues, indicating that these xenografts are poor representations of primary patient tissue (Fig. 2*A*). In addition, unsupervised hierarchical clustering also did not distinguish between the patient-matched benign or cancerous prostates, indicating that tyrosine phosphorylation remains relatively unchanged in treatment-naïve benign or cancerous prostates (Fig. 2*A* and Figs. S1 and S2). This suggests that evaluation of phosphotyrosine activity in metastatic CRPC tissues is crucial to testing potential new therapeutic treatments.

Phosphoproteomic Profiling and Kinase/Substrate Enrichment Analyses Identifies Several Druggable Nonmutated Kinase Targets and Pathways in Metastatic CRPC Lesions. Most patients with metastatic CRPC present with metastases at multiple sites, creating a therapeutic dilemma (15). We set out to examine heterogeneity in a cohort of metastatic CRPC patients including those with multiple, anatomically distinct metastatic sites for activated kinase targets. Several metastatic CRPC patients that we evaluated contained similar anatomic sites of involvement including tumors in the liver, lung, dura, and distant lymph nodes. Unsupervised hierarchical clustering of the tyrosine phosphorylation patterns of 10 metastatic lesions, including two patients for which we had two independent metastatic lesions, grouped samples by both patient and metastatic site (Fig. 2*B* and Fig. S3).

Phosphotyrosine peptide identification directly identified several activated kinases and phosphatases [tyrosine kinase 2 (TYK2) Y^{292}, protein tyrosine kinase 2 beta (PTK2B) Y^{579}, MAPK1/3 $Y^{187/204}$, discoidin domain receptor tyrosine kinase 1 (DDR1) Y^{796}, the JAK2/SRC kinase target STAT3 Y^{705}, and protein tyrosine phosphatase, non-receptor type 11 (PTPN11) $Y^{62/63}$]. Kinase–substrate relationship analyses, which predict kinase activity based on phosphopeptide motifs (8), have also identified putative upstream kinases and phosphatases [anaplastic lymphoma kinase (ALK), EGFR, PTK6, SRC, and PTPN2] that were active in individual metastatic CRPC samples (Figs. S1–S3 and Datasets S3–S5). These identifications were notable because of the US Food and Drug Administration–approved late-stage clinical trial of available kinase inhibitors targeting SRC (dasatinib/bosutinib/ponatinib) (16–18), EGFR (erlotinib) (19), ALK (crizotinib) (20), the MAPK1/3 upstream pathway kinases mitogen-activated protein kinase kinase 1/2 (MEK1/2) (trametinib) (21), or the STAT3 upstream kinase JAK2 (ruxolitinib) (22). Western blot analyses from five different patients confirmed the activation states of some of these kinases and also revealed interpatient heterogeneity as each patient evaluated displayed a unique phosphopattern (Fig. 2*C*). As expected, when evaluating prospectively the mutational status of a subset of our samples, we observed little to no activating mutations in these kinases. We did find one patient, RA57 Liver, to have two mutations [one in ephrin type-A receptor 4 (EPHA4) and one in mast/stem cell growth factor receptor (SCFR or KIT)] (6). However, our kinase/substrate enrichment scores did not predict kinase activity of either EPHA4 or KIT, again suggesting

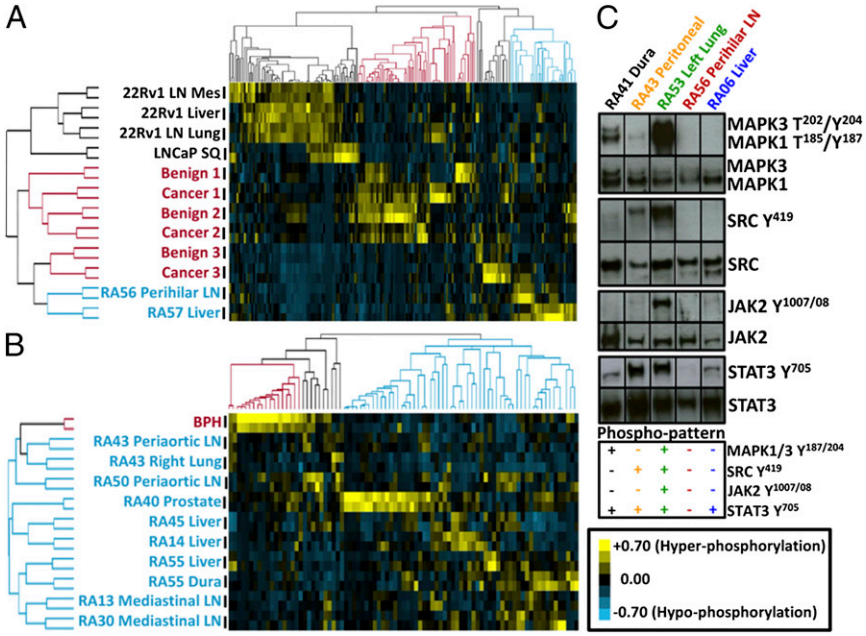

Fig. 2. Phosphoproteomic analyses of cell line-derived xenografts, treatment-naïve prostate cancer, and metastatic CRPC reveal distinct phosphopatterns. (*A*) Unsupervised hierarchical clustering of phosphotyrosine-enriched peptides separates cell line-derived xenograft tumors from primary prostate or metastatic tissue. (*B*) Further evaluation of a separate run of 10 metastatic CRPC lesions reveals patient-specific and metastatic site similarity of phosphotyrosine peptide patterns. (*C*) Western blot validation of four different activated kinases identified from both phosphoproteomics and inferred kinase activities confirms the heterogeneity observed across five different patients, as each patient exhibited a unique phosphopattern. Western blot data were separated to highlight each individual patient but were performed on the same western blot. Yellow, hyperphosphorylation; blue, hypophosphorylation. Intensity bar in Fig. 2*B* is applicable to Fig. 2*A*.

that these mutations did not lead to any detectable levels of activation of these kinases in this tissue sample.

Correlation analysis of the phosphotyrosine signaling patterns revealed a significant level of similarity in the phosphotyrosine profiles from lesions derived from a single patient, despite the fact that these lesions were derived from distinct anatomical sites (Fig. S4). Comparing three liver metastases, we also observed high levels of similarity between two of three lesions (Fig. S4). These MS–based phosphoproteomic data suggest that metastatic CRPC lesions isolated from the same patient may exhibit highly similar tyrosine kinase activation patterns but do not exclude the possibility that anatomical location may also drive similar phosphotyrosine signaling patterns in CRPC. This aspect is further analyzed below.

Large-Scale Analyses of Kinase Activation Patterns Reveals Intrapatient Similarity Across Multiple, Anatomically Distinct Metastases. To determine if signaling patterns were more similar within anatomically distinct metastatic lesions from the same CRPC patient or within sites of metastasis, we examined a larger, independent set of patients that included 28 distinct metastatic lesions from seven different CRPC patients (Fig. S5). Western blot analysis of phosphoproteins identified by MS and kinase/substrate enrichment analysis or the activated states of receptor tyrosine kinase (RTK) targets [EGFR Y^{1173}, ERBB2 Y^{1221}, and hepatocyte growth factor receptor (HGFR or MET) Y^{1234}] for which there are clinical inhibitors available confirmed our initial observation of intrapatient similarities (Fig. 3 and Fig. S6 *A*–*C*). Comparison of different patients revealed dramatically different kinase activation patterns. This ranged from SRC Y^{419}, STAT3 Y^{705}, MAPK1/3 $T^{185/202}/Y^{187/204}$, and AKT S^{473}, activated upon phosphatase and tensin homolog (*PTEN*) loss in the majority of prostate cancers, for patient RA43 to only STAT3 Y^{705} for patient RA55 (Fig. 3). These unique phosphopatterns suggest that shared kinase activities exist in metastatic CRPC lesions isolated from the same patient.

To determine if this pattern of intrapatient similarity across metastases remains consistent with a larger set of other RTK and intracellular kinases, we evaluated five previously analyzed sets of patient metastases using RTK and phosphokinase arrays from R&D Systems. Analysis of three or four anatomically distinct metastatic lesions from each patient revealed signaling patterns that were qualitatively similar within a patient's set of metastatic lesions (Fig. 4*A*). Patient-specific patterns included (*i*) tyrosine phosphorylation of ALK, RYK, and the activation site of AKT T^{308} in patient RA37; (*ii*) hemopoietic cell kinase (HCK) pY^{411} from patient RA56; and (*iii*) cellular RET (c-RET) phosphorylation in RA33 (Fig. 4*A*). Quantitation of these arrays revealed intrapatient similarities for nine phospho- and total proteins (Fig. 4*B*). Principal component analysis (PCA) of the kinases and proteins with detectable phosphorylation or expression ($n = 11$) demonstrated highly similar intrapatient grouping (Fig. 4*C* and Fig. S7). Surprisingly, the signaling patterns found in these metastatic lesions appear to be substantially cell autonomous as lesions from similar anatomical sites did not group together (Fig. 4*D*). Statistical analysis of pairwise correlation coefficients confirmed that metastatic CRPC lesions isolated from the same patient have strongly similar signaling patterns, more so than lesions from similar anatomical sites in different patients (Fig. S8).

Phosphorylation of Neuronal RTK RET in Metastatic CRPC Lesions with a Small Cell Neuroendocrine Carcinoma Phenotype. Further evaluation of the phospho-RTK arrays revealed tyrosine phosphorylation of RET in patient RA33 (Fig. 3*A*). RET is expressed in neuronal cell types, suggesting this patient may have suffered from a rare small cell neuroendocrine carcinoma (SCNC) phenotype (23). Indeed histological analyses of patient RA33 confirmed SCNC as evidenced by a diffuse, solid growth pattern with darkly stained nucleus, a homogeneous chromatin pattern, high nuclear/cytoplasmic (N/C) ratio, lack of nucleoli, and frequent mitotic figures (Fig. S9 *A* and *B*, arrows). These are in sharp contrast

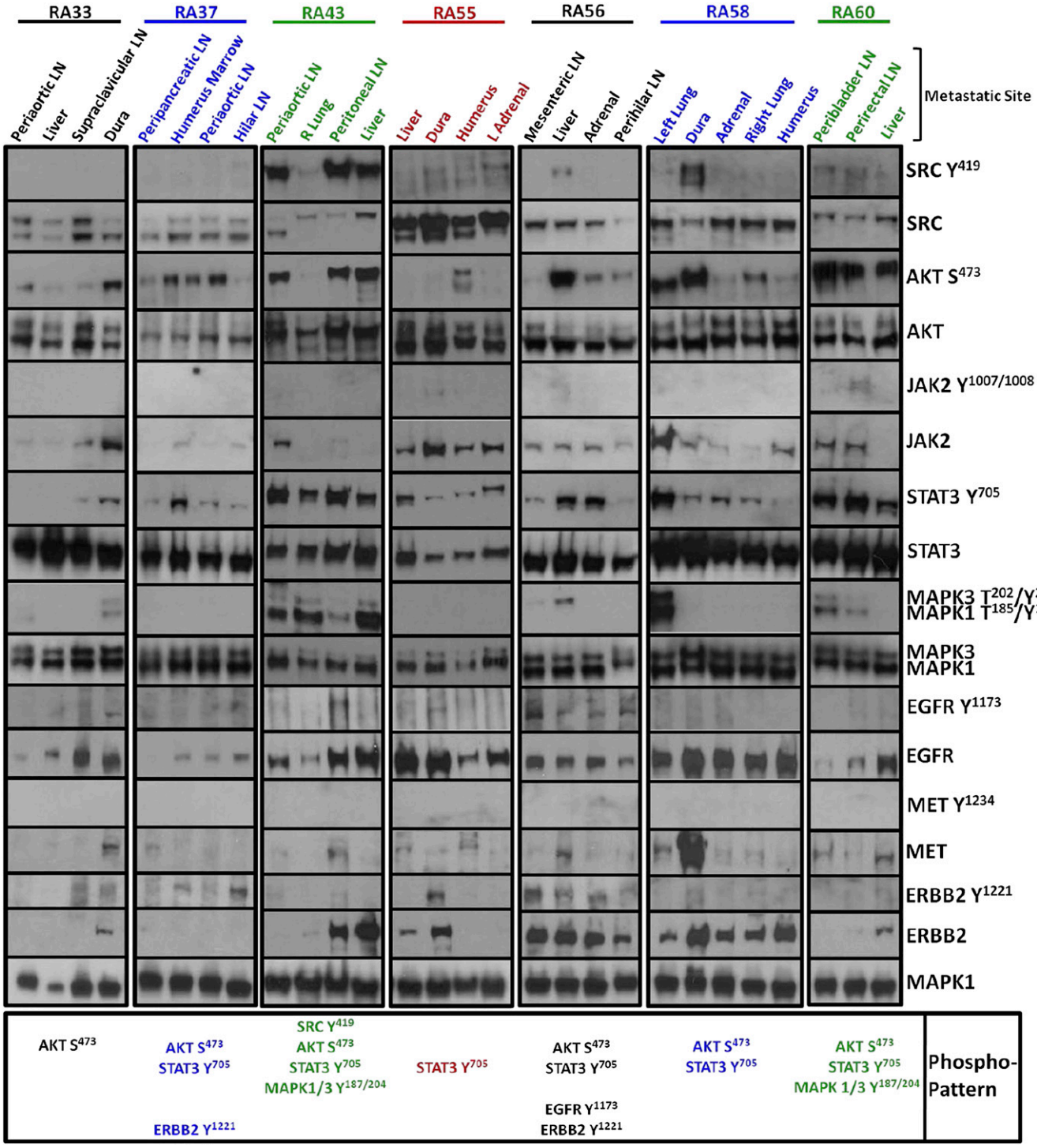

Fig. 3. Related phosphokinase and substrate expression patterns are observed within distinct anatomical metastatic lesions of the same patient. Western blot analyses from seven different sets of patients with three or four distinct metastatic lesions were evaluated for kinase activation patterns that were identified in the phosphoproteomic datasets and kinase–substrate relationships or RTKs that have been previously targeted clinically. Each patient expressed similar activated kinase patterns independent of the anatomical location of the metastatic lesions. The unique phosphopatterns are also depicted schematically below the Western blot data.

to the conventional prostatic adenocarcinoma that shows glandular formation (Fig. S9*C*, dashed circle), nuclear morphology consisting of open and vesicular chromatin patterns, and prominent nuclei (Fig. S9*C*, arrow). These data suggest that the molecular phenotyping of SCNC, as indicated by phospho-RET activity, may drive novel therapeutic strategies for this rarer subtype of prostate cancer.

Stratification of Metastatic CRPC Patients' Kinase Activation Patterns Suggests That Simultaneous Targeting of SRC and MEK Kinases May Be of Potential Therapeutic Value. To predict potential kinase inhibitor combination therapies for metastatic CRPC patients, we evaluated all 16 individual metastatic CRPC lesions that had been analyzed by phosphoproteomics. We pooled kinases that were

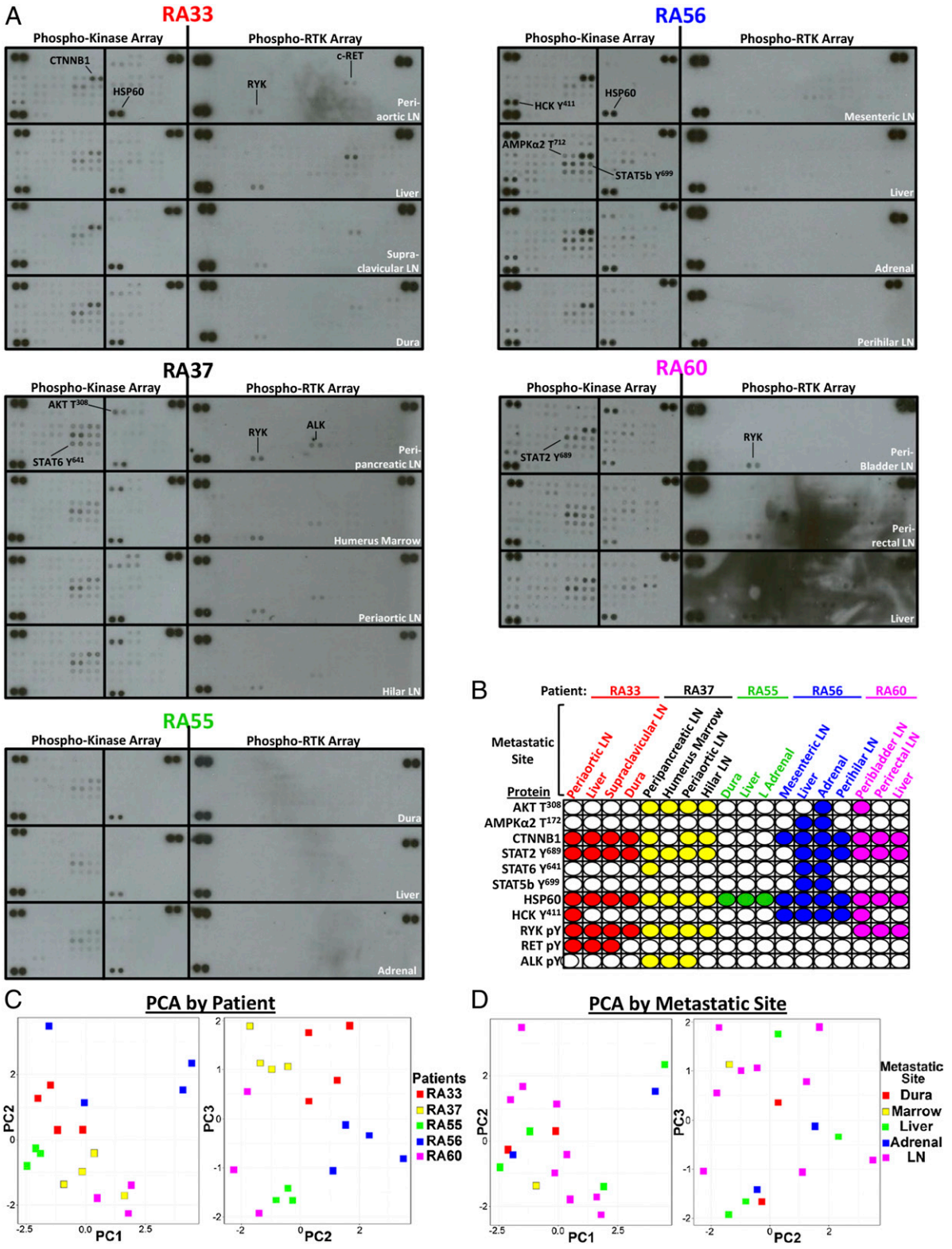

Fig. 4. Large-scale analyses of kinase activation patterns confirm intrapatient similarity across multiple, anatomically distinct metastases. (*A*) Phosphokinase and phospho-RTK arrays were used to analyze metastatic lesions from five different patients from anatomically distinct metastatic lesions. (*B*) Unique phosphopatterns were observed for each patient, and similar patterns were observed within the same patient, as shown with like-colored circles. Each observable phospho- or total protein spot from the phosphokinase and RTK arrays were used for PCA. LN, lymph node. (*C*) PCA analysis of all five patients confirms intrapatient kinase expression similarity and interpatient dissimilarity. (*D*) Grouping metastatic lesions by similar anatomical site shows no significant grouping of samples. Each phosphokinase and phospho-RTK array are spotted in duplicate, and positive control spots are located in the top left, right, and bottom left of each array. The first three principal components represent 77% of the total variance. Adrenal, adrenal gland lesions; LN, distant lymph node lesions; marrow, bone marrow lesion.

Table 1. Kinase and inhibitor stratification of metastatic CRPC patients

Patient number and metastatic location	Identified kinases via MS and western blot plus inferred kinases via kinase–substrate relationships*	Potential clinical inhibitors				
		Dasatinib†	Erlotinib‡	Crizotinib§	Ruxolitinib¶	Trametinib‖
RA06 Liver	EPHA3-7, SRC, PDGFR	X				
RA13 Mediastinal LN	ALK, FLT3/CSF1R/KIT, INSR, MAPK1, MAP3K2, PTK6, SRC	X		X		X
RA14 Liver	EGFR, MAPK1, MAP3K2, PTK6	X	X			X
RA30 Mediastinal LN	ALK, FLT3/CSF1R/KIT, MAP3K2, PTK6, SRC	X		X		X
RA40 Prostate	EGFR, MAPK1/3, MAP2K2, MAP3K2, PTK6, SRC	X	X			X
RA41 Dura	FLT3/CSF1R/KIT, MAPK1/3, SRC	X				X
RA43 Peritoneal and Right Lung	ALK, EGFR, EPHA3-7, MAPK1/3, PTK6, SRC	X	X	X		X
RA43 Periaortic LN	MAPK1/3, SRC	X				X
RA43 Right Lung	EGFR, FLT3/CSF1R/KIT, MAPK1/3, MAP2K2	X	X			X
RA45 Liver	ALK, MAP3K2			X		X
RA50 Periaortic LN	MAPK1/3, MAP3K2					X
RA53 Left Femur and Left Lung	ALK, EPHA3-7, JAK2, MAPK1/3, PDGFR, PTK6, SRC	X		X	X	X
RA55 Liver	ALK, EGFR, EPHA3, MAPK1/3, MAP2K2, MAP3K2, PTK6	X	X	X		X
RA55 Dura	EGFR, PTK6	X	X			
RA56 Perihilar LN	EGFR, HCK, TYK2	X	X		X	
RA57 Liver	EPHA7, MAP3K2, TYK2	X			X	X

*Kinases corresponding to identified phosphopeptides observed as >twofold over benign tissues, via western blotting, or kinase–substrate relationships ($P < 0.1$) as shown in Dataset S4.
†SRC family kinase, KIT, PDGFR, and EPHA receptor inhibitor.
‡EGFR inhibitor.
§ALK inhibitor.
¶JAK2 inhibitor.
‖MEK inhibitor.

identified from MS, western blot, and predicted kinase–substrate relationships to reveal a wide range of predicted kinase activities across the patient samples (Table 1). Mapping clinically available inhibitors to these kinases revealed 11 different TKI combinations with overlap between four sets of inhibitor combinations (Table 1). Notably, the SRC inhibitor dasatinib and the MEK inhibitor trametinib were predicted therapeutic strategies in 14 of 16 (87.5%) or 13 of 16 (81.2%) patients, respectively. If we consider combination therapy, 11 of 16 (68.8%) patients would be predicted to benefit from both SRC and MEK inhibitors, whereas 5 of 16 (31.2%) patients would not. There are no current clinical trials in prostate cancer evaluating the efficacy of SRC and MEK combination therapy in metastatic CRPC, but if initiated, stratification of patients based on activation of these two kinases would be necessary. Overall, the kinases identified in metastatic CRPC patients using phosphoproteomic analyses (*i*) may guide the molecular stratification of patients to direct the proper course of treatment with kinase inhibitor combinations, (*ii*) confirm the complexity observed across patients, and (*iii*) suggest that individualized therapy needs to be considered before clinical treatment decisions.

Discussion

From our study, we were able to measure protein phosphorylation in 41 metastatic CRPC samples from 17 patients including 16 samples by quantitative phosphotyrosine MS. Our phosphokinase profiling and evaluation of active kinases suggests that kinase activity patterns are patient-specific and are maintained across multiple metastatic lesions within the same patient. These data support previous studies suggesting that metastatic disease arises from a single precursor cancer cell or focal mass located at the primary tumor site (6, 12–14). Our findings add actionable information to this perspective. Kinase inhibitor treatment regimens guided by the biopsy of a single accessible metastatic lesion may be sufficient to predict the responses of multiple sites, leading to a more efficacious use of single agents or multidrug combinations, although this concept is still untested.

The development of new targeted therapies for metastatic CRPC presents a number of clinical questions. Major challenges include effective stratification of patients who will benefit from selected treatments and recognition of context-specific molecular targets. One approach to address these issues is the serial sampling and molecular characterization of malignant tissue from patients during the course of their disease. The increasing availability of high-throughput tools has enabled the genomic and transcriptomic profiling of large numbers of clinical carcinoma samples of different subtypes (4, 24, 25). Phosphoproteomic technology, particularly mass spectroscopy–based proteomics, is also rapidly advancing and has recently been applied to the elucidation of tyrosine-kinase–driven pathways in cell lines (26–29) or the discovery of activated kinases that may be useful for therapy in human cancers (30, 31).

Our analysis of phosphotyrosine signaling patterns in primary tumors and xenografts indicates that the prostate cell line-derived xenografts evaluated have different phosphorylation patterns compared with primary tissues. Supporting this notion, gene expression studies in small-cell lung cancer (SCLC) also identified primary tumor-specific signatures that were lost upon transitioning to cell culture (32), and proteomic analyses in colorectal cancer suggest that xenograft tumors are dramatically different from their cell line counterparts (33). This suggests that the stratification and prioritization of therapeutic targets for CRPC will require analysis of primary tissue, rather than cell lines or cell line-derived xenografts.

Interestingly, very few patient sets were positive for the activated states of EGFR, ERBB2, or MET, although they were detected in prostate cancer cell lines. Drugs targeting EGFR and ERBB2 did not produce significant results in CRPC patients (34,

35), however the MET inhibitor cabozantinib has shown promise in the clinic (36). This is in contrast to our observation that MET activity is not detected in our analyzed metastatic CRPC tissues. One explanation is that our sampling of metastatic CRPC tissues is too small or that MET activity was lost before tissue collection and we were not able to detect it. Two other possibilities are that cabozantinib activity in metastatic CRPC is not targeted toward epithelial MET but rather to MET expressed in osteoblasts or other mesenchymal cells in the bone microenvironment (36) and that cabozantinib is inhibiting another tyrosine kinase such as VEGFR2 or RET (37). Although we did not evaluate VEGFR2 activity, we did observe RET activity in SCNC, suggesting this kinase may be potentially targeted by cabozantinib in metastatic CRPC patients.

Rapid autopsy programs have paved the way for studies in genomic mutations, copy number alterations, and splicing variants from metastatic tissues that are otherwise difficult to obtain (4, 6, 15, 38, 39). Although we evaluated many soft tissue metastatic lesions, we were only able to evaluate five bone metastases. Although bone metastases are evident in over 90% of metastatic CRPC patients (15), metastatic bone tumors are hard to study because tumor material is lodged into hard, calcified bone, preventing the procurement of quality material for analysis. This is also especially difficult considering the large amount of tissue (>350 mg) required for phosphoproteomic preparations. A potential outcome could be that kinase patterns are principally determined by site of metastasis due to signals initiated by the surrounding local microenvironment creating a pre-metastatic niche (40). Tissue-specific kinase activation patterns were not observed in our study, but further evaluation of bone metastases in patients also harboring soft tissue metastases will be necessary to extend these findings.

Materials and Methods

Tissue Culture of Prostate Cancer Cell Lines and Derivation of Xenograft Tumors. 22Rv1 cells were grown in RPMI medium supplemented with L-glutamine, FBS, and nonessential amino acids (NEAAs). LNCaP, DU145, and C4-2 cells were grown in DMEM supplemented with L-glutamine, FBS, and NEAA. Thirty 15-cm plates were collected from each cell line and treated with 2 mM Vanadate for 30 min. Cells were subsequently lysed in 9 M Urea lysis buffer and used for phosphoproteomic analysis.

To generate metastatic tumors, 1×10^5 22Rv1 cells were injected intracardially as previously described, and dissemination was monitored using bioluminescence imaging (41). After 8 wks, tumors were extracted from the metastatic locations including the liver and lymph nodes in the mesenteric and lung regions. Also, to evaluate primary tumor growth, 1×10^6 LNCaP cells were injected s.c. and excised once they reached Division of Laboratory Animal Medicine (DLAM) limits.

Acquisition of Clinically Matched Benign and Cancerous Primary Prostate Tissues and Metastatic CRPC Samples. Patient samples were obtained from the University of California–Los Angeles (UCLA) Translational Pathology Core Laboratory, which is authorized by the UCLA Institutional Review Board to distribute anonymized tissues to researchers as described previously (42–44). Cancer and benign areas were clearly marked on the frozen section slides, and prostate tissue containing the cancer region was separated from the benign area before collecting for phosphoproteomic analyses.

The Rapid Autopsy program at the University of Michigan has been previously described (11, 39). Frozen tissues from the Rapid Autopsy program were sent overnight on dry ice for phosphotyrosine peptide analysis. Sections were stained with hematoxylin and eosin for representative histology.

Quantitative Analysis of Phosphotyrosine Peptides by MS. Tissue lysis was performed as previously described (8). Briefly, greater than 350 mg of frozen tumor mass was homogenized and sonicated in urea lysis buffer (20 mM Hepes pH 8.0, 9 M urea, 2.5 mM sodium pyrophosphate, 1.0 mM beta-glycerophosphate, 1% *N*-octyl glycoside, 2 mM sodium orthovanadate). Total protein was measured using the bicinchoninic acid (BCA) Protein Assay Kit (Thermo Scientific/Pierce), and 25 mg of total protein was used for phosphoproteomic analysis. The remaining protein lysate was frozen for subsequent western blot analyses.

Phosphotyrosine peptide enrichment and liquid chromatography tandem MS (LC-MS/MS) analysis was performed as previously described (8, 26, 45). Phosphopeptides were identified using the Proteome Discoverer software (version 1.4.0.88, Thermo Fisher Scientific). MS/MS fragmentation spectra were searched using SEQUEST against the Uniprot human reference proteome database with canonical and isoform sequences (downloaded January 2012 from uniprot.org). Search parameters included carbamidomethyl cysteine (*C) as a static modification. Dynamic modifications included phosphorylated tyrosine, serine, or threonine (pY, pS, and pT, respectively) and oxidized methionine (*M). The Percolator node of Protein Discoverer was used to calculate false discovery rate (FDR) thresholds, and the FDR for the datasets was adjusted to 1% (version 1.17, Thermo Scientific). The Percolator algorithm uses a target-decoy database search strategy and discriminates true and false identifications with a support vector machine (46). The PhosphoRS 2.0 node was used to more accurately localize the phosphate on the peptide (47). Only phosphopeptides with at least one phosphotyrosine assignment with a reported probability above 20% were considered. MS2 spectra for all reported phosphopeptides are deposited to the ProteomeXchange Consortium with the dataset identifier PXD000238 (48).

Data Analysis. Data analysis was performed as previously described (8). For clustering, we removed any peptides that had an ANOVA score greater than 0.2. Hierarchical clustering of phosphotyrosine data was performed using the Cluster program with the Pearson correlation and pairwise complete linkage analysis (49) and visualized using Java TreeView (50). Quantitative data for each phosphopeptide can be found in Dataset S5, *Batch 1–3*. To evaluate the significance of intrapatient and anatomical site similarity, the Pearson correlation coefficient was calculated for each pair of phosphotyrosine samples, and the resulting correlation matrix was clustered using the pHeatmap package in R. Statistical significance was assessed against the null hypothesis that the correlation was not different from zero.

Prediction of Kinase–Substrate Relationships and Enrichment Analysis of Kinase Activity. Predictions, enrichment, and permutation analyses have been previously described (8). Phosphotyrosine peptides were ranked by the signal-to-noise ratio observed for a given perturbation (e.g., metastatic CRPC compared with benign prostate or BPH). The enrichment scores for all putative upstream kinases are shown in Dataset S4, *Batch 1–3*.

Western Blot. For western blots, equal protein amounts of metastatic CRPC tissue urea lysates (20 or 30 μg) were used from tissues prepared as described previously (8). Antibodies were diluted as follows: AKT (1:1,000, Santa Cruz), pAKT S^{473} (1:2,000, Cell Signaling), EGFR (1:1,000, Cell Signaling), pEGFR Y^{1173} (1:1,000, Cell Signaling), STAT3 (1:1,000, Cell Signaling), pSTAT3 Y^{705} (1:2,000, Cell Signaling), JAK2 (1:1,000, Cell Signaling), pJAK2 $Y^{1007/1008}$ (1:500, Cell Signaling), MAPK1/3 (1:1,000, Cell Signaling), MAPK1/3 $T^{185/202}$/$Y^{187/204}$ (1:2,000, Cell Signaling), SRC (1:1,000, Millipore), pSRC Y^{419} (1:1,000, Cell Signaling), ERBB2 (1:1,000, Cell Signaling), pERBB2 $Y^{1221/1222}$ (1:1,000, Cell Signaling), MET (1:1,000, Cell Signaling), and pMET Y^{1234} (1:1,000, Cell Signaling). ECL substrate (Millipore) was used for detection and development on GE/Amersham film.

Phospho-RTK and Phosphokinase Arrays. Human Phospho-RTK (R&D Sytems) and phosphokinase (R&D Systems) arrays were used according to the manufacturer's instructions. Briefly, 300 μg of 9 M urea lysate for each metastatic sample was diluted in the kit-specific dilution buffer to a final concentration of 0.85 M urea and incubated with blocked membranes overnight. The membranes were washed and exposed to chemiluminescent reagent and developed on GE/Amersham film. Quantitation of each array was performed using Image J. To evaluate the significance of intrapatient and anatomical site similarity, the Pearson correlation coefficient was calculated for each pair of samples using only the kinases and proteins with detectable phosphorylation or expression (n = 11), and the correlation coefficients were clustered using the pHeatmap package in R. Statistical similarity of intrapatient lesions was assessed against the null hypothesis that the correlation was not different from zero. P values from multiple comparisons were combined using Fisher's Method where appropriate.

PCA. Each antibody-related spot on the Phospho-RTK and phosphokinase arrays was quantified using Image J. After background subtraction, the duplicate spots for each antibody were averaged, and antibodies with negligible signal were removed. The data were unit normalized, and principal components were calculated in R.

ACKNOWLEDGMENTS. We thank members of the O.N.W. laboratory for helpful comments and discussion on the manuscript. We thank Mireille Riedinger for purifying the 4G10 antibody used in mass spectrometry studies. We thank the Tissue Procurement Core Laboratory at UCLA for assistance on tissue processing and H&E staining. J.M.D. and T.S. are supported by the Department of Defense Prostate Cancer Research Program (W81XWH-11-1-0504 and W81XWH-12-1-0100, respectively). N.A.G. is supported by UCLA Scholars in Oncologic Molecular Imaging (SOMI) program, National Institutes of Health (NIH) Grant R25T CA098010. J.K.L. is supported by NIH Training Grant 5T32CA009297-28 and the UCLA Specialty Training and Advanced Research (STAR) Program. C.M.F. is supported by the UCLA Medical Scientist Training Program. J.H. is supported by the Department of Defense Prostate Cancer Research Program W81XWH-11-1-0227 and W81XWH-12-1-0206, UCLA Specialized Program in Research Excellence (SPORE) in prostate cancer, National Cancer Institute (NCI) 1R01CA158627, Stand Up to Cancer/AACR Dream Team Award, and Prostate Cancer Foundation Honorable A. David Mazzone Special Challenge Award. K.J.P. is supported by NIH U54 CA163124, NIH 1 U01CA143055-01A1, NIH 2 P50 CA69568, and NIH 1 PO1 CA093900 and receives support from the Prostate Cancer Foundation, the Taubman Research Institute as a Taubman Scholar, and the American Cancer Society as a Clinical Research Professor. T.G.G. is supported by NCI/NIH P01 CA168585 and R21 CA169993, American Cancer Society Research Scholar Award RSG-12-257-01-TBE, the CalTech–UCLA Joint Center for Translational Medicine, the UCLA Jonsson Cancer Center Foundation, the UCLA Institute for Molecular Medicine, the National Center for Advancing Translational Sciences UCLA Clinical and Translational Science Institute (CTSI) Grant UL1TR000124, and a Concern Fondation CONquer CanCER Now Award. J.H. and O.N.W. are supported by a Prostate Cancer Foundation Challenge Award. O.N.W. is an Investigator of the Howard Hughes Medical Institute and co–principal investigator of the West Coast Prostate Cancer Dream Team supported by Stand Up to Cancer/American Association for Cancer Research (AACR)/Prostate Cancer Foundation.

1. Kan Z, et al. (2010) Diverse somatic mutation patterns and pathway alterations in human cancers. *Nature* 466(7308):869–873.
2. Kim KS, et al. (2005) Predictors of the response to gefitinib in refractory non-small cell lung cancer. *Clin Cancer Res* 11(6):2244–2251.
3. Mass RD, et al. (2005) Evaluation of clinical outcomes according to HER2 detection by fluorescence in situ hybridization in women with metastatic breast cancer treated with trastuzumab. *Clin Breast Cancer* 6(3):240–246.
4. Taylor BS, et al. (2010) Integrative genomic profiling of human prostate cancer. *Cancer Cell* 18(1):11–22.
5. Kumar A, et al. (2011) Exome sequencing identifies a spectrum of mutation frequencies in advanced and lethal prostate cancers. *Proc Natl Acad Sci USA* 108(41): 17087–17092.
6. Grasso CS, et al. (2012) The mutational landscape of lethal castration-resistant prostate cancer. *Nature* 487(7406):239–243.
7. Cai H, Babic I, Wei X, Huang J, Witte ON (2011) Invasive prostate carcinoma driven by c-Src and androgen receptor synergy. *Cancer Res* 71(3):862–872.
8. Drake JM, et al. (2012) Oncogene-specific activation of tyrosine kinase networks during prostate cancer progression. *Proc Natl Acad Sci USA* 109(5):1643–1648.
9. Kuukasjärvi T, et al. (1997) Genetic heterogeneity and clonal evolution underlying development of asynchronous metastasis in human breast cancer. *Cancer Res* 57(8): 1597–1604.
10. Fidler IJ, Talmadge JE (1986) Evidence that intravenously derived murine pulmonary melanoma metastases can originate from the expansion of a single tumor cell. *Cancer Res* 46(10):5167–5171.
11. Shah RB, et al. (2004) Androgen-independent prostate cancer is a heterogeneous group of diseases: Lessons from a rapid autopsy program. *Cancer Res* 64(24):9209–9216.
12. Liu W, et al. (2009) Copy number analysis indicates monoclonal origin of lethal metastatic prostate cancer. *Nat Med* 15(5):559–565.
13. Aryee MJ, et al. (2013) DNA methylation alterations exhibit intraindividual stability and interindividual heterogeneity in prostate cancer metastases. *Sci Transl Med* 5(169):69ra10.
14. Mehra R, et al. (2008) Characterization of TMPRSS2-ETS gene aberrations in androgen-independent metastatic prostate cancer. *Cancer Res* 68(10):3584–3590.
15. Rubin MA, et al. (2000) Rapid ("warm") autopsy study for procurement of metastatic prostate cancer. *Clin Cancer Res* 6(3):1038–1045.
16. Cortes JE, et al. (2012) Bosutinib versus imatinib in newly diagnosed chronic-phase chronic myeloid leukemia: Results from the BELA trial. *J Clin Oncol* 30(28):3486–3492.
17. Cortes JE, et al. (2012) Ponatinib in refractory Philadelphia chromosome-positive leukemias. *N Engl J Med* 367(22):2075–2088.
18. Kantarjian H, et al. (2010) Dasatinib versus imatinib in newly diagnosed chronic-phase chronic myeloid leukemia. *N Engl J Med* 362(24):2260–2270.
19. Cohen MH, et al. (2010) Approval summary: Erlotinib maintenance therapy of advanced/metastatic non-small cell lung cancer (NSCLC). *Oncologist* 15(12):1344–1351.
20. O'Bryant CL, Wenger SD, Kim M, Thompson LA (2013) Crizotinib: A new treatment option for ALK-positive non-small cell lung cancer. *Ann Pharmacother* 47(2):189–197.
21. Flaherty KT, et al.; METRIC Study Group (2012) Improved survival with MEK inhibition in BRAF-mutated melanoma. *N Engl J Med* 367(2):107–114.
22. Mascarenhas J, Hoffman R (2012) Ruxolitinib: The first FDA approved therapy for the treatment of myelofibrosis. *Clin Cancer Res* 18(11):3008–3014.
23. Tai S, et al. (2011) PC3 is a cell line characteristic of prostatic small cell carcinoma. *Prostate* 71(15):1668–1679.
24. Anonymous; Cancer Genome Atlas Network (2012) Comprehensive molecular characterization of human colon and rectal cancer. *Nature* 487(7407):330–337.
25. Anonymous; Cancer Genome Atlas Network (2012) Comprehensive molecular portraits of human breast tumours. *Nature* 490(7418):61–70.
26. Rubbi L, et al. (2011) Global phosphoproteomics reveals crosstalk between Bcr-Abl and negative feedback mechanisms controlling Src signaling. *Sci Signal* 4(166):ra18.
27. Wolf-Yadlin A, et al. (2006) Effects of HER2 overexpression on cell signaling networks governing proliferation and migration. *Mol Syst Biol* 2:54.
28. Bai Y, et al. (2012) Phosphoproteomics identifies driver tyrosine kinases in sarcoma cell lines and tumors. *Cancer Res* 72(10):2501–2511.
29. Guha U, et al. (2008) Comparisons of tyrosine phosphorylated proteins in cells expressing lung cancer-specific alleles of EGFR and KRAS. *Proc Natl Acad Sci USA* 105(37):14112–14117.
30. Walters DK, et al. (2006) Activating alleles of JAK3 in acute megakaryoblastic leukemia. *Cancer Cell* 10(1):65–75.
31. Rikova K, et al. (2007) Global survey of phosphotyrosine signaling identifies oncogenic kinases in lung cancer. *Cell* 131(6):1190–1203.
32. Daniel VC, et al. (2009) A primary xenograft model of small-cell lung cancer reveals irreversible changes in gene expression imposed by culture in vitro. *Cancer Res* 69(8): 3364–3373.
33. Sirvent A, Vigy O, Orsetti B, Urbach S, Roche S (2012) Analysis of SRC oncogenic signaling in colorectal cancer by stable isotope labeling with heavy amino acids in mouse xenografts. *Mol Cell Proteomics* 11(12):1937–1950.
34. Nabhan C, et al. (2009) Erlotinib has moderate single-agent activity in chemotherapy-naïve castration-resistant prostate cancer: Final results of a phase II trial. *Urology* 74(3):665–671.
35. Ziada A, et al. (2004) The use of trastuzumab in the treatment of hormone refractory prostate cancer; phase II trial. *Prostate* 60(4):332–337.
36. Smith DC, et al. (2013) Cabozantinib in patients with advanced prostate cancer: Results of a phase II randomized discontinuation trial. *J Clin Oncol* 31(4):412–419.
37. Yakes FM, et al. (2011) Cabozantinib (XL184), a novel MET and VEGFR2 inhibitor, simultaneously suppresses metastasis, angiogenesis, and tumor growth. *Mol Cancer Ther* 10(12):2298–2308.
38. Friedlander TW, et al. (2012) Common structural and epigenetic changes in the genome of castration-resistant prostate cancer. *Cancer Res* 72(3):616–625.
39. Mehra R, et al. (2011) Characterization of bone metastases from rapid autopsies of prostate cancer patients. *Clin Cancer Res* 17(12):3924–3932.
40. Psaila B, Lyden D (2009) The metastatic niche: Adapting the foreign soil. *Nat Rev Cancer* 9(4):285–293.
41. Drake JM, Gabriel CL, Henry MD (2005) Assessing tumor growth and distribution in a model of prostate cancer metastasis using bioluminescence imaging. *Clin Exp Metastasis* 22(8):674–684.
42. Goldstein AS, et al. (2011) Purification and direct transformation of epithelial progenitor cells from primary human prostate. *Nat Protoc* 6(5):656–667.
43. Stoyanova T, et al. (2012) Regulated proteolysis of Trop2 drives epithelial hyperplasia and stem cell self-renewal via β-catenin signaling. *Genes Dev* 26(20):2271–2285.
44. Goldstein AS, Huang J, Guo C, Garraway IP, Witte ON (2010) Identification of a cell of origin for human prostate cancer. *Science* 329(5991):568–571.
45. Graham NA, et al. (2012) Glucose deprivation activates a metabolic and signaling amplification loop leading to cell death. *Mol Syst Biol* 8:589.
46. Spivak M, Weston J, Bottou L, Käll L, Noble WS (2009) Improvements to the percolator algorithm for Peptide identification from shotgun proteomics data sets. *J Proteome Res* 8(7):3737–3745.
47. Taus T, et al. (2011) Universal and confident phosphorylation site localization using phosphoRS. *J Proteome Res* 10(12):5354–5362.
48. Vizcaíno JA, et al. (2013) The PRoteomics IDEntifications (PRIDE) database and associated tools: Status in 2013. *Nucleic Acids Res* 41(Database issue):D1063–D1069.
49. Eisen MB, Spellman PT, Brown PO, Botstein D (1998) Cluster analysis and display of genome-wide expression patterns. *Proc Natl Acad Sci USA* 95(25):14863–14868.
50. Saldanha AJ (2004) Java Treeview—Extensible visualization of microarray data. *Bioinformatics* 20(17):3246–3248.